Chem Biol Drug Des 2012; **80:** 81–89

Research Article

doi: 10.1111/j.1747-0285.2012.01346.x

N-Nitrourea Derivatives as Novel Potential Fungicides against *Rhizoctonia solani*: Synthesis, Antifungal Activities, and 3D-QSAR

Xiufang Cao[1], Shengzhen Xu[1], Xuegang Li[1], Xiaoxia Shen[1], Qingye Zhang[1], Jianhong Li[2] and Changshui Chen[1,*]

[1]College of Science, Huazhong Agricultural University, Wuhan 430070, China

[2]Department of Plant Protection, Huazhong Agricultural University, Wuhan 430070, China

**Corresponding author: Changshui Chen, caoxiufang@mail.hzau.edu.cn*

A series of *N*-nitrourea derivatives bearing various aryl substituents were conveniently obtained *via* three steps including nitration, carbamic chlorination, and aminolysis reactions. The structures of all newly synthesized compounds were characterized and confirmed by IR, ^{1}H-NMR, MS, and elemental analysis. The preliminary bioassays indicate that five compounds possess sufficient fungicidal activity against *Rhizoctonia solani*. Structure–activity relationship (SAR) is also discussed based on the experimental data, and the further quantitative structure–activity relationship (QSAR) was analyzed using comparative molecular field analysis (CoMFA) and comparative molecular similarity indices analysis (CoMSIA).

Key words: antifungal activities, *N*-Nitrourea, quantitative structure–activity relationship, *Rhizoctonia solani*

Received 21 June 2011, revised 8 January 2012 and accepted for publication 8 January 2012

Rice sheath blight caused by *Rhizoctonia solani* is one of the most destructive rice diseases worldwide and severely impairs both rice yield and quality (1). Under conditions favorable for disease development, rice grain yield losses, ranging from 4% to 50%, have been attributed to sheath blight (2). In Japan, this disease causes a yield loss of as high as 20% and affects about 120 000–190 000 ha. In the United States, a yield loss of 50% is reported when susceptible cultivars are planted (3). In China, sheath blight disease affects about 15–20 million hectares and causes a yield loss of 6 million tons of rice grains per year (4). Therefore, the research on novel inhibitors controlling the *Rhizoctonia solani* becomes active, necessary, and meaningful.

Nowadays, urea derivatives have occupied a pivotal position in pesticide chemistry because of their significant activities (5–11), including herbicidal, antimicrobial, insecticidal activities, and so on. Many studies have proved that modification of both sides of carbamide bridge's amines is an effective way to obtain new analogues with higher activity. On the other hand, *N*-nitro-substituted anilines displayed broad-spectrum biological activities including herbicidal properties (12), antifungal effects (13), and plant growth regulating activities (14). Keeping these considerations in mind, we proposed that the urea derivatives bearing a new group nitro in the NH-CO-NH bridge should display some interesting biological activities.

As a continuation of our ongoing project aimed, we report herein the detailed synthetic procedures of series of *N*-nitrourea derivatives and bioassay results, and the further quantitative structure–activity relationships of these synthesized compounds were also analyzed using comparative molecular field analysis (CoMFA) (15) and comparative molecular similarity indices analysis (CoMSIA) (16,17). Fortunately, some compounds with promising fungicidal activities were identified.

Experimental Section

Instrumentation and chemicals

All reagents were commercially available, and all solvents and liquid reagents were dried by standard methods and distilled before use. Melting points were determined with a digital melting point apparatus and are uncorrected. IR spectra were recorded on a Thermo Nicolet FT-IR Avatar 330 instrument. ^{1}H-NMR spectra were measured on a Bruker AM spectrometer (Bruker, Fallanden, Switzerland) with tetramethylsilane as internal standard and DMSO-d_6 as solvent. Elemental analysis was performed on a Vario EL III Elemental analysis instrument (Elementar Analysensysteme GmbH, Hanau, Germany). The progress of the reactions was monitored by TLC on silica gel plates visualized with UV light.

General procedure for the preparation of target compounds 4–41

Preparation of compound **4–41**: Fuming nitric acid (16 mL) was slowly added dropwise to the stirred acetic anhydride (30 mL) for 30 min at 10–12 °C and kept stirring for 1 h. The formed crude product of acetyl nitrate **1** would be added dropwise to a solution of 2,4,6-trichloroaniline (50 g) in dry ethanoic acid (300 mL) and acetic anhydride (10 mL) for 1 h at 14 °C. The reaction mixture was stirred for another 1 h and then poured into ice water (2 L).The

precipitate **2** was filtered and washed with water (1 L), which was recrystallized from ethanol and dried in vacuo. Precipitate **2** (10 mmol) with 2 mL triethylamine was added dropwise to the BTC (3.3 mmol) toluene solution. The mixture was stirred at −5 °C for 1 h and then heated to 50 °C and kept reacting for 2 h. The intermediate **3** was formed and without isolated. After quenching the unreacted phosgene with dry nitrogen, a series of substituted anilines (The structure of various anilines are shown in Table 1) with 2 mL triethylamine were added dropwise to the unseparated product **3**, churned at 50–80 °C for 1–10 h, and then cooled to room temperature. The respective ureas **4–41** were precipitated, filtered, and washed with toluene, excess water, and acetone. Crude products were further purified by recrystallization (DMF/acetone).

N-nitro-*N*′-phenyl-*N*-(2,4,6-trichlorophenyl)urea (**4**): Ammonolysis at 50 °C for 4 h. Yield 63.7%, m.p. 229–230 °C; IR (KBr)/cm: 3267 (N-H), 3066 (Ar-H), 1646 (C=O), 1257 (N-NO_2). ^{1}H NMR (400 MHz, DMSO-d_6): δ 8.98 (s, 1H, NH), 7.76 (s, 2H, ArH), 7.45 (d, J = 8.0 Hz, 2H, ArH), 7.29 (d, J = 7.6 Hz, 2H, ArH), 6.99 (t, J = 7.6, 6.8 Hz, 1H, ArH). Anal. Calcd for $C_{13}H_8Cl_3N_3O_3$: C, 43.30; H, 2.24; N, 11.65; Found: C, 43.23; H, 2.12; N, 11.80.

Table 1: Structures and biological activities of the compounds used in training and test sets

Compounds	Ar	Yeild (%)	mp (°C)	IC_{50} (μg/mL)
4[a]	Phenyl	63.7	229–230	448
5	4-CH_3Ph	78.7	232–233	220
6	3-CH_3Ph	83.4	227–228	193
7	2-OCH_3Ph	70.6	235–237	567
8	4-NO_2Ph	48.4	286–288	106
9	2-NO_2Ph	46.1	273–274	149
10	4-OCH_3Ph	77.3	245–246	219
11	2-CH_3Ph	86.8	241–243	323
12	4-BrPh	59.3	244–245	121
13	4-FPh	69.7	223–225	170
14	1-Naphthyl	54.9	247–248	227
15	2,6-di-CH_3Ph	73.7	252–253	978
16	4-OC_2H_5Ph	57.1	267–269	239
17	2-OC_2H_5Ph	68.2	238–239	287
18	3-BrPh	53.6	258–260	119
19	3-Cl-4-FPh	50.1	242–245	133
20	2,4-di-BrPh	50.4	241–242	93
21[a]	2,4-di-FPh	62.6	238–239	104
22	3-F-4-CH_3Ph	76.6	245–246	107
23	3-Cl-4-CH_3Ph	72.5	241–242	72
24	3,4-di-CH_3Ph	76.8	242–244	84
25	3-NO_2-4-CH_3Ph	59.1	250–251	132
26	3,4-di-OCH_3Ph	50.2	237–238	105
27	2-FPh	69.4	233–234	44
28[a]	3-FPh	70.1	231–232	98
29[a]	3,5-di-CH_3Ph	82.4	242–244	59
30	3,5-di-ClPh	51.7	260–261	88
31[a]	3-CH_3-5-ClPh	72.6	259–261	100
32	2,4-di-ClPh	65.6	236–238	57
33	2-CH_3-3-ClPh	72.5	246–248	66
34[a]	2,4-di-CH_3Ph	78.1	249–251	189
35	2,5-di-CH_3Ph	75.5	236–238	125
36[a]	2,3-di-CH_3Ph	74.2	245–246	75
37	2,6-di-FPh	66.7	243–244	29
38	4-ClPh	58.5	278–279	30
39	3-ClPh	47.8	239–241	69
40[a]	2-ClPh	52.6	249–250	55
41	2-NO_2-4-ClPh	54.5	283–285	32

[a]Test set compounds mp (melting point, °C).

N′-(4-methylphenyl)-*N*-nitro-*N*-(2,4,6-trichlorophenyl)urea (**5**): Ammonolysis at 50 °C for 1 h. Yield 78.7%, m.p. 232–233 °C; IR (KBr)/cm: 3280 (N-H), 3079 (Ar-H), 2919 (C-H), 1654 (C=O), 1283 (N-NO_2); ^{1}H NMR (400 MHz, DMSO-d_6): δ 8.85 (s, 1H, NH), 7.75 (s, 2H, ArH), 7.32 (d, J = 6.4 Hz, 2H, ArH), 7.07(d, J = 6.8 Hz, 2H, ArH), 2.24 (s, 3H, CH_3). Anal. Calcd for $C_{14}H_{10}Cl_3N_3O_3$: C, 44.89; H, 2.69; N, 11.22; Found: C, 45.01; H, 2.64; N, 11.35.

N′-(3-methylphenyl)-*N*-nitro-*N*-(2,4,6-trichlorophenyl)urea (**6**): Ammonolysis at 50 °C for 2 h. Yield 83.4%, m.p. 227–228 °C; IR (KBr)/cm: 3280 (N-H), 3076 (Ar-H), 2916 (C-H), 1644 (C=O), 1284 (N-NO_2); ^{1}H NMR (400 MHz, DMSO-d_6): δ 8.89 (s, 1H, NH), 7.75 (s, 2H, ArH), 7.29 (s, 1H, ArH), 7.22 (d, J = 8.4 Hz, 1H, ArH), 7.15 (t, J = 7.2, 6.0 Hz, 1H, ArH), 6.79 (d, J = 7.6 Hz, 1H, ArH), 2.26 (s, 3H, CH_3). Anal. Calcd for $C_{14}H_{10}Cl_3N_3O_3$: C, 44.89; H, 2.69; N, 11.22; Found: C, 44.99; H, 2.63; N, 11.34.

N′-(2-methoxyphenyl)-*N*-nitro-*N*-(2,4,6-trichlorophenyl)urea (**7**): Ammonolysis at 50 °C for 4 h. Yield 70.6%, m.p. 235–237 °C; IR (KBr)/cm: 3304 (N-H), 3079 (Ar-H), 2835 (C-H), 1660 (C=O), 1220 (N-NO_2). ^{1}H NMR (400 MHz, DMSO-d_6): δ 8.93 (s, 1H, NH), 8.05 (d, J = 8.4 Hz, 1H, ArH), 7.74 (s, 2H, ArH), 7.01 (d, J = 7.6 Hz, 1H, ArH), 6.90–6.98 (m, 1H, ArH), 6.86 (d, J = 8.4 Hz, 1H, ArH), 3.88 (s, 3H, OCH_3). Anal. Calcd for : $C_{14}H_{10}Cl_3N_3O_4$ C, 43.05; H, 2.58; N, 10.76; Found: C, 43.14; H, 2.42; N, 10.88.

N-nitro-*N*′-(4-nitrophenyl)-*N*-(2,4,6-trichlorophenyl)urea (**8**): Ammonolysis at 80 °C for 10 h. Yield 48.4%, m.p. 286–288 °C; IR (KBr)/cm: 3281 (N-H), 3080 (Ar-H), 1656 (C=O), 1373 (N-NO_2). ^{1}H NMR (400 MHz, DMSO-d_6): δ 10.04 (s, 1H, NH), 8.02 (d, J = 8.4 Hz, 2H, ArH), 7.69 (d, J = 8.4 Hz, 2H, ArH), 7.28 (s, 2H, ArH). Anal. Calcd for $C_{13}H_7Cl_3N_4O_5$: C, 38.50; H, 1.74; N, 13.81; Found: C, 38.43; H, 1.87; N, 13.62.

N-nitro-*N*′-(2-nitrophenyl)-*N*-(2,4,6-trichlorophenyl)urea (**9**): Ammonolysis at 80 °C for 10 h. Yield 46.1%, m.p. 273–274 °C; IR (KBr)/cm: 3295 (N-H), 3082 (Ar-H), 1658 (C=O), 1338 (N-NO_2). ^{1}H NMR (400 MHz, DMSO-d_6): δ 9.42 (s, 1H, NH), 8.52 (t, J = 9.6, 2.4 Hz, 1H, ArH), 8.47 (d, J = 8.6 Hz, 1H, ArH), 8.35 (d, J = 3.2 Hz, 1H, ArH), 8.18 (t, J = 8.8, 3.6 Hz, 1H, ArH), 7.77 (s, 2H, ArH). Anal. Calcd for $C_{13}H_7Cl_3N_4O_5$: C, 38.50; H, 1.74; N, 13.81; Found: C, 38.44; H, 1.89; N, 13.65.

N′-(4-methoxyphenyl)-*N*-nitro-*N*-(2,4,6-trichlorophenyl)urea (**10**): Ammonolysis at 50 °C for 4 h. Yield 77.3%, m.p. 245–246 °C; IR (KBr)/cm: 3281 (N-H), 3078 (Ar-H), 2834 (C-H), 1645 (C=O), 1250 (N-NO_2). ^{1}H NMR (400 MHz, DMSO-d_6): δ 8.75 (s, 1H, NH), 7.72 (s, 2H, ArH), 7.33 (d, J = 8.8 Hz, 2H, ArH), 6.84 (d, J = 8.8 Hz, 2H, ArH), 3.69 (s, 3H, OCH_3). Anal. Calcd for $C_{14}H_{10}Cl_3N_3O_4$: C, 43.05; H, 2.58; N, 10.76; Found: C, 43.16; H, 2.44; N, 10.90.

N'-(2-methylphenyl)-*N*-nitro-*N*-(2,4,6-trichlorophenyl)urea (**11**): Ammonolysis at 50 °C for 2 h. Yield 86.8%, m.p. 241–243 °C; IR (KBr)/cm: 3267 (N-H), 3067 (Ar-H), 2972 (C-H), 1647 (C=O), 1286 (N-NO_2); ^{1}H NMR (400 MHz, DMSO-d_6): δ 8.87 (s, 1H, NH), 7.75 (s, 2H, ArH), 7.21 (d, J = 6.4 Hz, 1H, ArH), 7.13–7.20 (m, 1H, ArH), 6.96–7.08 (m, 1H, ArH), 6.81 (d, J = 8.0 Hz, 1H, ArH), 2.23 (s, 3H, CH_3). Anal. Calcd for $C_{14}H_{10}Cl_3N_3O_3$: C, 44.89; H, 2.69; N, 11.22; Found: C, 45.01; H, 2.57; N, 11.32.

N'-(4-bromophenyl)-*N*-nitro-*N*-(2,4,6-trichlorophenyl)urea (**12**): Ammonolysis at 60 °C for 5 h. Yield 59.3%, m.p. 244–245 °C; IR (KBr)/cm: 3275 (N-H), 3078 (Ar-H), 1653 (C=O), 1278 (N-NO_2); ^{1}H NMR(400 MHz, DMSO-d_6): δ 9.13 (s, 1H, NH), 7.86 (d, J = 7.6 Hz, 2H, ArH), 7.75 (d, J = 6.4 Hz,2H, ArH), 7.43 (s, 2H, ArH). Anal. Calcd for $C_{13}H_7BrCl_3N_3O_3$: C, 35.53; H, 1.61; N, 9.56; Found: C, 35.64; H, 1.73; N, 9.82.

N'-(4-fluorophenyl)-*N*-nitro-*N*-(2,4,6-trichlorophenyl)urea (**13**): Ammonolysis at 60 °C for 4 h. Yield 69.7%, m.p. 223–225 °C; IR (KBr)/cm: 3314 (N-H), 3081 (Ar-H), 1669 (C=O), 1270 (N-NO_2). ^{1}H NMR (400 MHz, DMSO-d_6): δ 8.30 (s, 1H, NH), 7.73 (s, 2H, ArH), 7.30–7.47 (m, 2H, ArH), 7.08 (t, J = 8.8 Hz, 2H, ArH). Anal. Calcd for $C_{13}H_7Cl_3FN_3O_3$: C, 41.24; H, 1.86; N, 11.10; Found: C, 41.33; H, 1.94; N, 11.25.

N'-1-naphthyl-*N*-nitro-*N*-(2,4,6-trichlorophenyl)urea (**14**): Ammonolysis at 70 °C for 5 h. Yield 54.9%, m.p. 247–248 °C; IR (KBr)/cm: 3269 (N-H), 3049 (Ar-H), 1646 (C=O), 1267 (N-NO_2); ^{1}H NMR (400 MHz, DMSO-d_6): δ 9.04 (s, 1H, NH), 8.15 (d, J = 8.0 Hz, 1H, ArH), 7.93 (t, J = 6.4, 7.6 Hz, 2H, ArH), 7.67 (s, 2H, ArH), 7.50–7.66 (m, 3H, ArH), 7.47 (t, J = 7.6, 8.0 Hz, 1H, ArH). Anal. Calcd for $C_{17}H_{10}Cl_3N_3O_3$: C, 49.72; H, 2.45; N, 10.23; Found: C, 49.66; H, 2.38; N, 10.33.

N'-(2,6-dimethylphenyl)-*N*-nitro-*N*-(2,4,6-trichlorophenyl)urea (**15**): Ammonolysis at 50 °C for 1 h. Yield 73.7%, m.p. 252–253 °C; IR (KBr)/cm: 3274 (N-H), 3070 (Ar-H), 2974 (C-H), 2921 (C-H), 1646 (C=O), 1264 (N-NO_2); ^{1}H NMR (400 MHz, DMSO-d_6): δ 8.33 (s, 1H, NH), 7.72 (s, 2H, ArH), 7.06 (d, J = 4.0 Hz, 2H, ArH), 6.85 (t, J = 6.8, 7.2 Hz, 1H, ArH), 2.23 (s, 6H, -CH_3). Anal. Calcd for $C_{15}H_{12}Cl_3N_3O_3$: C, 46.36; H, 3.11; N, 10.81; Found: C, 46.44; H, 3.22; N, 10.95.

N'-(4-ethoxyphenyl)-*N*-nitro-*N*-(2,4,6-trichlorophenyl)urea (**16**): Ammonolysis at 60 °C for 2 h. Yield 57.1%, m.p. 267–269 °C; IR (KBr)/cm: 3273 (N-H), 3076 (Ar-H), 2977 (C-H), 1642 (C=O), 1246 (N-NO_2); ^{1}H NMR (400 MHz, DMSO-d_6): δ 8.75 (s, 1H, NH), 7.74 (s, 2H, ArH), 7.33 (d, J = 9.2 Hz, 2H, ArH), 6.84 (d, J = 8.8 Hz, 2H, ArH), 3.96 (m, 2H, -CH_2), 1.30 (t, J = 7.2, 6.8 Hz, 3H, -CH_3). Anal. Calcd for $C_{15}H_{12}Cl_3N_3O_4$: C, 44.52; H, 2.99; N, 10.38; Found: C, 44.61; H, 3.10; N, 10.48.

N'-(2-ethoxyphenyl)-*N*-nitro-*N*-(2,4,6-trichlorophenyl)urea (**17**): Ammonolysis at 60 °C for 2 h. Yield 68.2%, m.p. 238–239 °C; IR (KBr)/cm: 3291 (N-H), 3072 (Ar-H), 2979 (C-H), 1645 (C=O), 1263 (N-NO_2); ^{1}H NMR (400 MHz, DMSO-d_6): δ 9.08 (s, 1H, NH), 8.06 (d, J = 7.6 Hz, 1H, ArH), 7.76 (s, 2H, ArH), 7.01 (d, J = 8.0 Hz, 1H, ArH), 6.92 (q, J = 1.2, 6.4, 8.0 Hz, 1H, ArH), 6.85 (t, J = 8.0, 7.2 Hz, 1H, ArH), 4.14 (q, J = 6.8, 7.2, 6.8 Hz, 2H, CH_2), 1.42 (t, J = 6.8, 7.2 Hz, 3H, CH_3). Anal. Calcd for $C_{15}H_{12}Cl_3N_3O_4$: C, 44.52; H, 2.99; N, 10.38; Found: C, 44.64; H, 3.11; N, 10.49.

N'-(3-bromophenyl)-*N*-nitro-*N*-(2,4,6-trichlorophenyl)urea (**18**): Ammonolysis at 60 °C for 5 h. Yield 53.6%, m.p. 258–260 °C; IR (KBr) cm-1: 3277 (N-H), 3075 (Ar-H), 1641 (C=O), 1274 (N-NO_2); ^{1}H NMR (400 MHz, DMSO-d_6): δ 9.19 (s, 1H, NH), 8.35 (s, 1H, ArH), 7.78 (s, 2H, ArH), 7.34 (d, J = 7.6 Hz, 1H, ArH), 7.23 (t, J = 8.0 Hz, 1H, ArH), 7.15 (d, J = 7.2 Hz, 1H, ArH). Anal. Calcd for $C_{13}H_7BrCl_3N_3O_3$: C, 35.53; H, 1.61; N, 9.56; Found: C, 35.62; H, 1.70; N, 9.81.

N'-(3-chloro-4-fluorophenyl)-*N*-nitro-*N*-(2,4,6-trichlorophenyl)urea(**19**): Ammonolysis at 70 °C for 7 h. Yield 50.1%, m.p. 242–245 °C; IR (KBr)/cm: 3309 (N-H), 3084 (Ar-H), 1650 (C=O), 1263 (N-NO_2); ^{1}H NMR (400 MHz, DMSO-d_6): δ 9.20 (s, 1H, NH), 8.38 (s, 1H, ArH), 7.77 (s, 2H, ArH), 7.33 (d, J = 7.2 Hz, 2H, ArH). Anal. Calcd for $C_{13}H_6Cl_4FN_3O_3$: C, 37.80; H, 1.46; N, 10.17; Found: C, 37.89; H, 1.63; N, 10.31.

N'-(2,4-dibromophenyl)-*N*-nitro-*N*-(2,4,6-trichlorophenyl)urea (**20**): Ammonolysis at 80 °C for 6 h. Yield 50.4%, m.p. 241–242 °C; IR (KBr)/cm: 3288 (N-H), 3081 (Ar-H), 1650 (C=O), 1284 (N-NO_2); ^{1}H NMR (400 MHz, DMSO-d_6): δ 9.19 (s, 1H, NH), 8.01 (s, 1H, ArH), 7.90 (d, J = 6.0 Hz, 1H, ArH), 7.87 (s, 2H, ArH), 7.54 (d, J = 8.8 Hz, 1H, ArH). Anal. Calcd for $C_{13}H_6Br_2Cl_3N_3O_3$: C, 30.12; H, 1.17; N, 8.11; Found: C, 30.23; H, 1.09; N, 8.30.

N'-(3,4-difluorophenyl)-*N*-nitro-*N*-(2,4,6-trichlorophenyl)urea (**21**): Ammonolysis at 50 °C for 4 h. Yield 62.6%, m.p. 238–239 °C; IR (KBr)/cm: 3271 (N-H), 3084 (Ar-H), 1650 (C=O), 1250 (N-NO_2); ^{1}H NMR (400 MHz, DMSO-d_6): δ 9.20 (s, 1H, NH), 8.34 (s, 2H, ArH), 7.74 (s, 1H, ArH), 7.60 (d, J = 6.8 Hz,1H, ArH), 7.27 (d, J = 6.4 Hz,1H, ArH). Anal. Calcd for $C_{13}H_6Cl_3F_2N_3O_3$: C, 39.37; H, 1.53; N, 10.60; Found: C, 39.53; H, 1.62; N, 10.81.

N'-(3-fluoro-4-methylphenyl)-*N*-nitro-*N*-(2,4,6-trichlorophenyl)urea (**22**): Ammonolysis at 50 °C for 2 h. Yield 76.6%, m.p. 245–246 °C; IR (KBr)/cm: 3280 (N-H), 3076 (Ar-H), 2921 (C-H), 1655 (C=O), 1274 (N-NO_2); ^{1}H NMR (400 MHz, DMSO-d_6): δ 9.10 (s, 1H, NH), 8.28 (s, 2H, ArH), 7.76 (s, 1H, ArH), 7.73 (d, J = 6.0 Hz,1H, ArH), 7.04 (d, J = 6.4 Hz, 1H, ArH), 2.16 (s, 3H, CH_3). Anal. Calcd for $C_{14}H_9Cl_3FN_3O_3$: C, 42.83; H, 2.31; N, 10.70; Found: C, 42.93; H, 2.18; N, 10.84.

N'-(3-chloro-4-methylphenyl)-*N*-nitro-*N*-(2,4,6-trichlorophenyl)urea (**23**): Ammonolysis at 70 °C for 3 h. Yield 72.5%, m.p. 241–242 °C; IR (KBr)/cm: 3279 (N-H), 3080 (Ar-H), 2914 (C-H), 1652 (C=O), 1283 (N-NO_2); ^{1}H NMR (400 MHz, DMSO-d_6): δ 9.32 (s, 1H, NH), 8.55 (s, 2H, ArH), 8.00 (s, 1H, ArH), 7.91 (d, J = 6.8 Hz,1H, ArH), 7.46 (d, J = 6.0 Hz, 1H, ArH), 2.49 (s, 3H, CH_3). Anal. Calcd for $C_{14}H_9Cl_4N_3O_3$: C, 41.11; H, 2.22; N, 10.27; Found: C, 41.24; H, 2.12; N, 10.42.

N'-(3,4-dimethylphenyl)-*N*-nitro-*N*-(2,4,6-trichlorophenyl)urea (**24**): Ammonolysis at 50 °C for 2 h. Yield 76.8%, m.p. 242–244 °C; IR (KBr)/cm: 3280 (N-H), 3074 (Ar-H), 2921 (C-H), 1654 (C=O), 1267 (N-NO_2); ^{1}H NMR (400 MHz, DMSO-d_6): δ 8.75 (s, 1H, NH), 7.74 (s, 2H, ArH), 7.22 (s, 1H, ArH), 7.14 (d, J = 5.6 Hz,1H, ArH), 7.00 (d,

J = 4.8 Hz, 1H, ArH), 2.17 (s, 3H, CH_3), 2.15 (s, 3H, CH_3). Anal. Calcd for $C_{15}H_{12}Cl_3N_3O_3$: C, 46.36; H, 3.11; N, 10.81; Found: C, 46.27; H, 3.19; N, 10.98.

N′-(4-methyl-3-nitrophenyl)-*N*-nitro-*N*-(2,4,6-trichlorophenyl)urea (**25**): Ammonolysis at 80 °C for 5 h. Yield 59.1%, m.p. 250–251 °C; IR (KBr)/cm: 3313 (N-H), 3076 (Ar-H), 2989 (C-H), 1654 (C=O), 1310 (N-NO_2); ^{1}H NMR (400 MHz, DMSO-d_6): δ 9.40 (s, 1H, NH), 8.44 (s, 2H, ArH), 7.77 (s, 1H, ArH), 7.56 (d, *J* = 7.2 Hz,1H, ArH), 7.41 (d, *J* = 6.8 Hz, 1H, ArH), 2.45 (s, 3H, CH_3). Anal. Calcd for $C_{14}H_9Cl_3N_4O_5$: C, 40.07; H, 2.16; N, 13.35; Found: C, 40.16; H,2.10; N, 13.46.

N′-(3,4-dimethoxyphenyl)-*N*-nitro-*N*-(2,4,6-trichlorophenyl)urea (**26**): Ammonolysis at 80 °C for 5 h. Yield 50.2%, m.p. 237–238 °C; IR (KBr)/cm: 3283 (N-H), 3077 (Ar-H), 2993 (C-H), 1644 (C=O), 1238 (N-NO_2); ^{1}H NMR (400 MHz, DMSO-d_6): δ 9.24 (s, 1H, NH), 8.19 (s, 2H, ArH), 7.48 (s, 1H, ArH), 7.25 (d, *J* = 7.6 Hz,1H, ArH), 7.06 (d, *J* = 7.2 Hz, 1H, ArH), 4.05 (s, 3H, CH_3), 4.03 (s, 3H, CH_3). Anal. Calcd for $C_{15}H_{12}Cl_3N_3O_5$: C, 42.83; H, 2.88; N, 9.99; Found: C, 42.94; H,2.98; N, 10.10.

N′-(2-fluorophenyl)-*N*-nitro-*N*-(2,4,6-trichlorophenyl)urea (**27**): Ammonolysis at 50 °C for 3 h. Yield 69.4%, m.p. 233–234 °C; IR (KBr)/cm: 3270 (N-H), 3076 (Ar-H), 1652 (C=O), 1273 (N-NO_2); ^{1}H NMR (400 MHz, DMSO-d_6): δ 8.85 (s, 1H, NH), 8.63 (s, 2H, ArH), 8.05 (d, *J* = 7.2 Hz, 1H, ArH), 7.14–7.29 (m, 1H, ArH), 7.0–7.14 (m, 1H, ArH), 6.98 (d, *J* = 6.0 Hz, 1H, ArH). Anal. Calcd for $C_{13}H_7Cl_3FN_3O_3$: C, 41.24; H, 1.86; N, 11.10; Found: C, 41.31; H, 1.80; N, 11.22.

N′-(3-fluorophenyl)-*N*-nitro-*N*-(2,4,6-trichlorophenyl)urea (**28**): Ammonolysis at 50 °C for 3 h. Yield 70.1%, m.p. 231–232 °C; IR (KBr)/cm: 3277 (N-H), 3083 (Ar-H), 1655 (C=O), 1277 (N-NO_2); ^{1}H NMR (400 MHz, DMSO-d_6): δ 9.24 (s, 1H, NH), 8.33 (s, 2H, ArH), 7.76 (s, 1H, ArH), 7.43 (d, *J* = 6.0 Hz, 1H, ArH), 7.28 (t, *J* = 7.6, 6.4 Hz, 1H, ArH), 7.14 (d, *J* = 7.2 Hz, 1H, ArH). Anal. Calcd for $C_{13}H_7Cl_3FN_3O_3$: C, 41.24; H, 1.86; N, 11.10; Found: C, 41.32; H, 1.82; N, 11.24.

N′-(3,5-dimethylphenyl)-*N*-nitro-*N*-(2,4,6-trichlorophenyl)urea (**29**): Ammonolysis at 50 °C for 1 h. Yield 82.4%, m.p. 242–244 °C; IR (KBr)/cm: 3276 (N-H), 3077 (Ar-H), 3014 (Ar-H), 2917 (C-H), 1648 (C=O), 1278 (N-NO_2); ^{1}H NMR (400 MHz, DMSO-d_6): δ 8.75 (s, 1H, NH), 8.14 (s, 2H, ArH), 7.74 (s, 2H, ArH), 7.02 (s, 1H, ArH), 2.17 (s, 6H, CH_3). Anal. Calcd for $C_{15}H_{12}Cl_3N_3O_3$: C, 46.36; H, 3.11; N, 10.81; Found: C, 46.27; H, 3.19; N, 10.98.

N′-(3,5-dichlorophenyl)-*N*-nitro-*N*-(2,4,6-trichlorophenyl)urea (**30**): Ammonolysis at 80 °C for 5 h. Yield 51.7%, m.p. 260–261 °C; IR (KBr)/cm: 3275 (N-H), 3079 (Ar-H), 1649 (C=O), 1268 (N-NO_2); ^{1}H NMR (400 MHz, DMSO-d_6): δ 9.39 (s, 1H, NH), 8.53 (s, 2H, ArH), 7.78 (s, 1H, ArH), 7.56 (s, 2H, ArH). Anal. Calcd for $C_{13}H_6Cl_5N_3O_3$: C, 36.36; H, 1.41; N, 9.78; Found: C, 36.44; H, 1.52; N, 9.95.

N′-(3-chloro-5-methylphenyl)-*N*-nitro-*N*-(2,4,6-trichlorophenyl)urea (**31**): Ammonolysis at 70 °C for 3 h. Yield 72.6%, m.p. 259–261 °C; IR (KBr)/cm: 3274 (N-H), 3079 (Ar-H), 1644 (C=O), 1267 (N-NO_2); ^{1}H NMR (400 MHz, DMSO-d_6): δ 8.59 (s, 1H, NH), 7.75 (s, 2H, ArH), 7.64 (s, 1H, ArH), 7.18 (s, 2H, ArH), 2.30 (s, 3H, CH_3). Anal. Calcd for $C_{14}H_9Cl_4N_3O_3$: C, 41.11; H, 2.22; N, 10.27; Found: C, 41.20; H, 2.14; N, 10.42.

N′-(2,4-dichlorophenyl)-*N*-nitro-*N*-(2,4,6-trichlorophenyl)urea (**32**): Ammonolysis at 80 °C for 8 h. Yield 65.6%, m.p. 236–238 °C; IR (KBr)/cm: 3283 (N-H), 3080 (Ar-H), 1658 (C=O), 1279 (N-NO_2); ^{1}H NMR (400 MHz, DMSO-d_6): δ 8.55 (s, 1H, NH), 7.74 (s, 2H, ArH), 7.56 (s, 2H, ArH), 7.05 (d, *J* = 6.4 Hz, 1H, ArH), 6.78 (d, *J* = 8.0 Hz, 1H, ArH); GC-MS (DMSO) m/z(%): 427(1), 282(50). Anal. Calcd for $C_{13}H_6Cl_5N_3O_3$: C, 36.36; H, 1.41; N, 9.78; Found: C, 36.42; H, 1.52; N, 9.96.

N′-(3-chloro-2-methylphenyl)-*N*-nitro-*N*-(2,4,6-trichlorophenyl)urea (**33**): Ammonolysis at 60 °C for 4 h. Yield 72.5%, m.p. 246–248 °C; IR (KBr)/cm: 3279 (N-H), 3078 (Ar-H), 1650 (C=O), 1271 (N-NO_2); ^{1}H NMR (400 MHz, DMSO-d_6): δ 8.59 (s, 1H, NH), 7.75 (s, 2H, ArH), 7.56–7.69 (m, 1H, ArH), 7.10–7.19 (m, 2H, ArH), 2.30 (s, 3H, CH_3); GC-MS (DMSO) m/z(%): 407 (1), 281(57), 91(72). Anal. Calcd for $C_{14}H_9Cl_4N_3O_3$: C, 41.11; H, 2.22; N, 10.27; Found: C, 41.21; H, 2.33; N, 10.43.

N′-(2,4-dimethylphenyl)-*N*-nitro-*N*-(2,4,6-trichlorophenyl)urea (**34**): Ammonolysis at 50 °C for 4 h. Yield 78.1%, m.p. 249–251 °C; IR (KBr)/cm: 3280 (N-H), 3078 (Ar-H), 2919 (C-H), 1651 (C=O), 1269 (N-NO_2); ^{1}H NMR (400 MHz, DMSO-d_6): δ 8.46 (s, 1H, NH), 7.73 (s, 2H, ArH), 7.53 (d, *J* = 6.8 Hz, 1H, ArH), 6.99 (s, 1H, ArH), 6.93 (d, *J* = 6.0 Hz, 1H, ArH), 2.22 (s, 3H, CH_3), 2.21 (s, 3H, CH_3); GC-MS (DMSO) m/z(%): 387(2), 359(4), 282(63), 91(28). Anal. Calcd for $C_{15}H_{12}Cl_3N_3O_3$: C, 46.36; H, 3.11; N, 10.81; Found: C, 46.26; H, 3.22; N, 10.97.

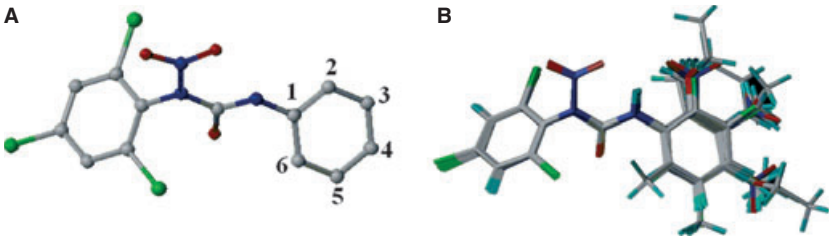

Figure 1: Structure of *N*-nitro urea derivatives: (A) General structure for title compounds; (B) 3D view of all the aligned molecules in training and test sets.

N'-(2,5-dimethylphenyl)-*N*-nitro-*N*-(2,4,6-trichlorophenyl)urea (**35**): Ammonolysis at 50 °C for 4 h. Yield 75.5%, m.p. 236–238 °C; IR (KBr)/cm: 3284 (N-H), 3077 (Ar-H), 2921 (C-H), 1648 (C=O), 1283 (N-NO_2); ^{1}H NMR (400 MHz, DMSO-d_6): δ 8.55 (s, 1H, NH), 7.74 (s, 2H, ArH), 7.57 (s, 1H, ArH), 7.05 (d, J = 6.4 Hz, 1H, ArH), 6.78 (d, J = 6.0 Hz, 1H, ArH), 2.22 (s, 3H, CH_3), 2.20 (s, 3H, CH_3); GC-MS (DMSO) m/z(%): 387(2), 281(57), 91(42). Anal. Calcd for $C_{15}H_{12}Cl_3N_3O_3$: C, 46.36; H, 3.11; N, 10.81; Found: C, 46.24; H, 3.21; N, 10.99.

N'-(2,3-dimethylphenyl)-*N*-nitro-*N*-(2,4,6-trichlorophenyl)urea (**36**): Ammonolysis at 50 °C for 4 h. Yield 74.2%, m.p. 245–246 °C; IR (KBr)/cm: 3288 (N-H), 3067 (Ar-H), 2956 (C-H), 1648 (C=O), 1273 (N-NO_2); ^{1}H NMR (400 MHz, DMSO-d_6): δ 8.44 (s, 1H, NH), 7.73 (s, 2H, ArH), 7.43 (d, J = 7.2 Hz, 1H, ArH), 7.02 (t, J = 6.4, 6.8 Hz, 1H, ArH), 6.92 (d, J = 6.4 Hz, 1H, ArH), 2.25 (s, 3H, CH_3), 2.15 (s, 3H, CH_3); GC-MS (DMSO) m/z(%): 387(2), 282(85), 9(25). Anal. Calcd for $C_{15}H_{12}Cl_3N_3O_3$: C, 46.36; H, 3.11; N, 10.81; Found: C, 46.25; H, 3.22; N, 10.97.

N'-(2,6-difluorophenyl)-*N*-nitro-*N*-(2,4,6-trichlorophenyl)urea (**37**): Ammonolysis at 60 °C for 5 h. Yield 66.7%, m.p. 243–244 °C; IR (KBr)/cm: 3282 (N-H), 3071 (Ar-H), 1661 (C=O), 1243 (N-NO_2); ^{1}H NMR (400 MHz, DMSO-d_6): δ 8.50 (s, 1H, NH), 7.74 (s, 2H, ArH), 7.22–7.35 (m, 1H, ArH), 7.04–7.20 (m, 2H, ArH); GC-MS (DMSO) m/z(%): 395(1), 282(38), 45(100). Anal. Calcd for $C_{13}H_6Cl_3F_2N_3O_3$: C, 39.37; H, 1.53; N, 10.60; Found: C, 39.28; H, 1.59; N, 10.81.

N'-(4-chlorophenyl)-*N*-nitro-*N*-(2,4,6-trichlorophenyl)urea (**38**): Ammonolysis at 80 °C for 5 h. Yield 58.5%, m.p. 278–279 °C; IR (KBr)/cm: 3293 (N-H), 3075 (Ar-H), 1655 (C=O), 1279 (N-NO_2). ^{1}H NMR (400 MHz, DMSO-d_6): δ 8.86 (s, 1H, NH), 7.77 (s, 2H, ArH), 7.47 (d, J = 8.0 Hz, 2H, ArH), 7.32 (d, J = 8.0 Hz, 2H, ArH). Anal. Calcd for $C_{13}H_7Cl_4N_3O_3$: C, 39.53; H, 1.79; N, 10.64; Found: C, 39.43; H, 1.88; N, 10.82.

N'-(3-chlorophenyl)-*N*-nitro-*N*-(2,4,6-trichlorophenyl)urea (**39**): Ammonolysis at 80 °C for 5 h. Yield 47.6%, m.p. 239–241 °C; IR (KBr)/cm: 3273 (N-H), 3078 (Ar-H), 1641 (C=O), 1274 (N-NO_2); ^{1}H NMR (400 MHz, DMSO-d_6): δ 9.31 (s, 1H, NH), 8.42 (s, 1H, ArH), 7.76 (s, 2H, ArH), 7.67 (d, J = 5.6 Hz, 1H, ArH), 7.27 (d, J = 7.2 Hz, 1H, ArH), 7.00–7.08 (m, 1H, ArH). Anal. Calcd for $C_{13}H_7Cl_4N_3O_3$: C, 39.53; H, 1.79; N, 10.64; Found: C, 39.42; H, 1.89; N, 10.81.

N'-(2-methylphenyl)-*N*-nitro-*N*-(2,4,6-trichlorophenyl)urea (**40**): Ammonolysis at 80 °C for 5 h. Yield 52.6%, m.p. 249–250 °C; IR (KBr)/cm: 3273 (N-H), 3077 (Ar-H), 1653 (C=O), 1290 (N-NO_2). ^{1}H NMR (400 MHz, DMSO-d_6): δ 8.86 (s, 1H, NH), 7.77 (t, J = 8.8, 9.6 Hz, 1H, ArH), 7.65 (s, 2H, ArH), 7.37 (d, J = 8.4 Hz, 1H, ArH), 7.22 (d, J = 8.8 Hz, 1H, ArH), 7.13 (d, J = 4.8, 5.2 Hz, 1H, ArH). Anal. Calcd for $C_{14}H_{10}Cl_3N_3O_3$: C, 44.89; H, 2.69; N, 11.22; Found: C, 45.01; H, 2.80; N, 11.37.

N'-(4-chloro-2-nitrophenyl)-*N*-nitro-*N*-(2,4,6-trichlorophenyl)urea (**41**): Ammonolysis at 80 °C for 10 h. Yield 54.5%, m.p. 283–285 °C; IR (KBr)/cm: 3314 (N-H), 3081 (Ar-H), 1669 (C=O), 1270 (N-NO_2). ^{1}H NMR (400 MHz, DMSO-d_6): δ 9.65 (s, 1H, NH), 8.75 (s, 1H, ArH), 8.30 (d, J = 8.8 Hz, 1H, ArH), 8.13 (d, J = 2.4 Hz, 1H, ArH), 7.77 (s,

Table 2: CoMFA and CoMSIA results

	LOO		NV		
Fields	q^2	*N*	r^2	SEE	*F*
CoMFA					
Both steric and electrostatic	**0.773**	**4**	**0.959**	**0.077**	**146.833**
Steric	0.729	3	0.902	0.117	79.975
Electrostatic	0.480	2	0.762	0.179	43.160
CoMSIA					
Steric	0.615	6	0.869	0.143	25.488
Electrostatic	0.522	6	0.889	0.132	30.758
Hydrophobic	0.260	4	0.669	0.219	12.649
H-bond donor	0.492	2	0.629	0.223	22.907
H-bond acceptor	0.350	5	0.659	0.226	9.293
Steric, electrostatic	**0.720**	**6**	**0.936**	**0.100**	**56.051**
H-bond donor, H-bond acceptor	0.499	5	0.694	0.215	10.803

Note: *N* is the optimal number of components, NV is No-Validation, q^2 is the leave-one-out (LOO) cross-validation coefficient, r^2 is the non-cross-validation coefficient, SEE is the standard error of estimation, and *F* is the *F*-test value. The best models are marked in bold.

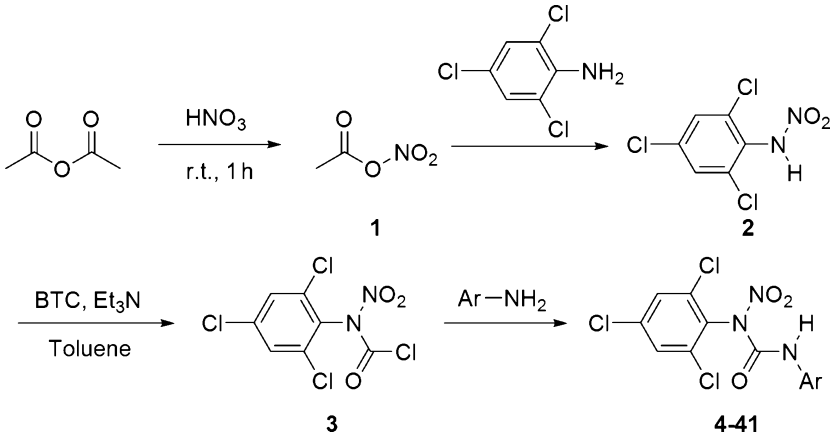

Scheme 1: Synthetic route for target compounds **4–41** and the structure of $ArNH_2$ are shown in Table 1.

2H, ArH). Anal. Calcd for $C_{13}H_6Cl_4N_4O_5$: C, 35.48; H, 1.37; N, 12.73; Found: C, 35.37; H, 1.54; N, 12.89.

Antifungal activities

The *in vivo* fungicidal activities of *N*-nitrourea derivatives were tested against *Rhizoctonia solani* by the modified agar cup method according to the reported method in literature (18).

Molecular modeling

The 38 target compounds were divided into a training set and a testing set as shown in Table 1. The IC_{50} values were converted into pIC_{50} (-log IC_{50}) for use in 3D-QSAR analysis. CoMFA and CoMSIA study was performed using SYBYL 7.3 molecular modeling software (19). The 3D structures of all compounds were sketched by the Build/Edit module of SYBYL7.3. Partial atomic charges were calculated by the Gasteiger–Huckel method, and energy minimizations were performed by using the Tripos force and the Powell conjugate gradient algorithm with a convergence criterion of 0.05kcal/(mol Å) (20,21). The potent compound **41** was chosen as the template. The common substructure is displayed in Figure 1. Each compound in the training and testing sets was aligned to the template using the database alignment function because of its easy implementation and effectiveness. The aligned compounds are shown in Figure 1.

A grid that extends 4 Å units beyond the dimensions of aligned molecules was established (22). The CoMFA steric and electrostatic fields were calculated at grid points using Tripos Standard with a default energy cutoff of 30 kcal/mol. For CoMSIA, steric, electrostatic, hydrophobic, hydrogen-bond donor, and acceptor fields were evaluated using probe atom with +1 charge, radius of 1 Å, and +1 hydrophobicity on the same lattice as the CoMFA used. Each single and some possible combinations of fields were calculated. The relationship between activity data and fields of training set was analyzed by partial least squares (PLS) methods (23,24). The leave-one-out (LOO) cross-validation was performed to determine optimum number of components (M) and cross-validated coefficient q^2, which indicates the consistency and prediction of models for the training set. Then, no validation was performed to derive the final PLS regression models, and the results were shown in Table 2.

The external predictive ability of the models can be measured by R^2_{pred}, R^2_{pred} was according to the formula: $R^2_{pred} = (SD - PRESS)/SD$, where SD is the sum of the squared deviations between the biological activities of the test set compounds and mean activity of the training set compounds and PRESS is the sum of squared deviations between experimental and predicted activities of the test set compounds (25).

Results and Discussion

Synthesis

The synthetic route for target compounds **4–41** is outlined in Scheme 1. According to the reported procedures (26), 2,4,6-trichloroaniline was nitrified by acetyl nitrate **1** to give the *N*-nitro-*N*-(2, 4, 6-trichlorophenyl)amine **2** in yields of 75–86%. Then, at the presence of triethylamine as base (27), a subsequent reaction of BTC and intermediate **2** produced nitro (2,4,6-trichlorophenyl) carbamic chloride **3**. Without further isolation, the key intermediate **3** reacted with the corresponding amine to afford the compounds **4–41** in the yields of 45–87%.

In vivo antifungal activities

Thirty-eight *N*-nitrourea derivatives **4–41** were synchronously tested the *in vivo* fungicidal activities against *Rhizoctonia solani* by agar cup method (18). As shown in Table 1, Compounds **20**, **23**,

Table 3: Observed and predicted activities for training and test sets' compounds by 3D-QSAR models

		CoMFA model		CoMSIA model	
Compounds	Observed pIC50	Predicted	Residual	Predicted	Residual
Training set					
5	3.66	3.66	0.00	3.61	−0.05
6	3.71	3.74	0.03	3.65	−0.06
7	3.24	3.28	0.04	3.23	−0.01
8	3.98	4.03	0.05	3.91	−0.07
9	3.83	3.73	−0.10	3.86	0.03
10	3.66	3.57	−0.09	3.55	−0.11
11	3.49	3.55	0.06	3.56	0.07
12	3.92	3.96	0.04	3.89	−0.03
13	3.76	3.77	0.01	3.89	0.13
14	3.64	3.69	0.05	3.59	−0.05
15	3.01	2.94	−0.07	2.98	−0.03
16	3.62	3.62	0.00	3.69	0.07
17	3.55	3.53	−0.02	3.60	0.05
18	3.92	3.95	0.03	3.98	0.06
19	3.88	3.86	−0.02	3.99	0.11
20	4.03	4.00	−0.03	3.99	−0.04
22	3.97	3.97	0.00	4.05	0.08
23	4.14	4.07	−0.07	4.06	−0.08
24	4.08	4.12	0.04	4.17	0.09
25	3.88	4.00	0.12	3.91	0.03
26	3.98	4.02	0.04	4.02	0.04
27	4.36	4.38	0.02	4.38	0.02
30	4.05	4.11	0.06	4.13	0.08
32	4.24	4.26	0.02	4.27	0.03
33	4.18	4.10	−0.08	3.98	−0.20
35	3.90	3.98	0.08	4.02	0.12
37	4.54	4.51	−0.03	4.48	−0.06
38	4.53	4.27	−0.26	4.28	−0.25
39	4.16	4.16	0.00	4.23	0.07
41	4.49	4.52	0.03	4.44	−0.05
Test set					
4[a]	3.35	3.60	0.25	3.58	0.23
21[a]	3.92	3.79	−0.13	4.00	0.08
28[a]	4.10	4.24	0.14	4.35	0.25
29[a]	4.23	4.04	−0.19	4.41	0.18
31[a]	4.00	4.03	0.03	4.21	0.21
34[a]	3.72	4.00	0.28	4.01	0.29
36[a]	4.12	4.16	0.04	4.06	−0.06
40[a]	4.26	4.17	−0.09	4.25	−0.01
Average			0.14		0.16

[a]The selective compounds as test set compounds.

24, **32**, **33**, and **39** display good activities, as the IC_{50} are less than 100 μg/mL. Compounds **27**, **37**, **38**, **40**, and **41** exhibit good antifungal activities with lower IC_{50} below 50 μg/mL.

For structure–activity relationship (SAR), the biological data obtained the various substituents on *N*′-benzene ring displayed different activities. For mono-substituted compounds, **27** (2-F) >**40** (2-Cl) > **9** (2-NO_2) > **17** (2-OC_2H_5) > **11** (2-CH_3) > **7** (2-OCH_3); **39** (3-Cl) > **28** (3-F) > **18** (3-Br) > **6** (3-CH_3); **38** (4-Cl) > **8** (4-NO_2) > **13** (4-F) > **10** (4-OCH_3) > **5** (4-CH_3) > **16** (4-OC_2H_5). Most of the disubstituted compounds displayed good antifungal activities. Their IC_{50} values are all under 150 μg/mL except compound **15** (2,6-di-CH_3, 978 μg/mL) and **34** (2,4-di-CH_3, 189 μg/mL). In addition, the compounds with optimal activity are **41** (2-NO_2-4-Cl, 32 μg/mL) and **37** (2,6-di-F, 29 μg/mL).

Structure–activity relationships

The statistical results of the 3D-QSAR models are summarized in the Table 2, in which the best models are marked in bold. As seen, both the CoMFA (q^2 = 0.773, r^2 = 0.959) and CoMSIA (q^2 = 0.720, r^2 = 0.936) models show good prediction capability.

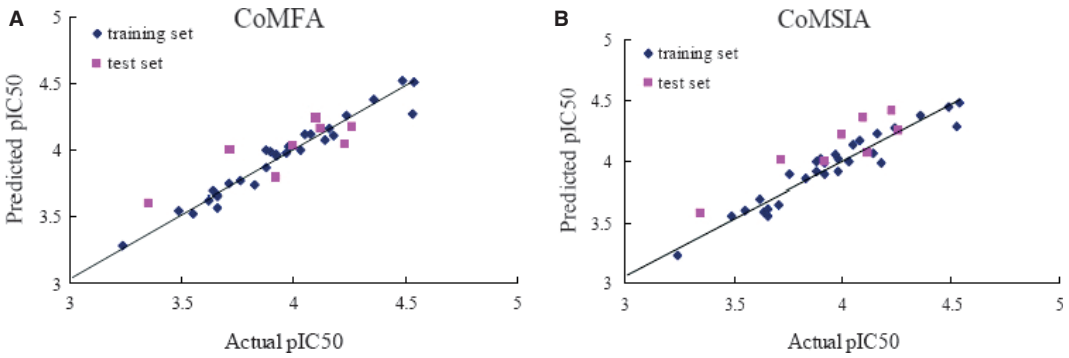

Figure 2: Plot of the predicted versus observed pIC_{50} values for all the molecules based on CoMFA (q^2 = 0.773, r^2 = 0.959) model (A) and CoMSIA (q^2 = 0.720, r^2 = 0.936) model (B).

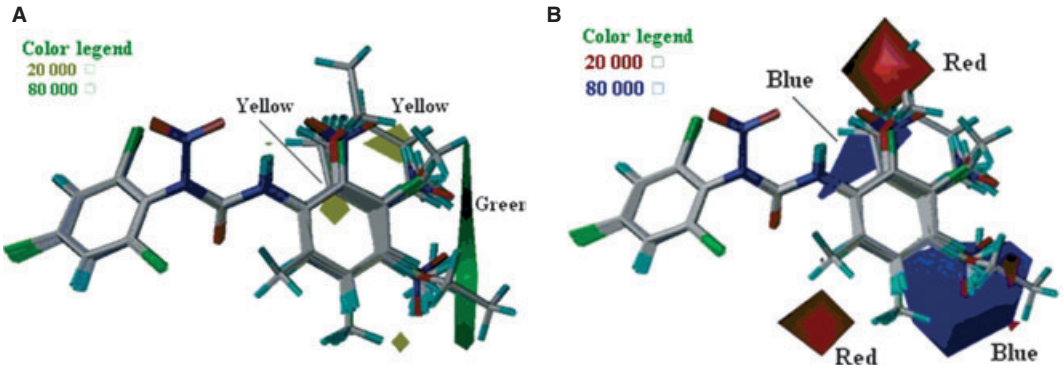

Figure 3: CoMFA contour maps: (A) steric contour map; (B) electrostatic contour map.

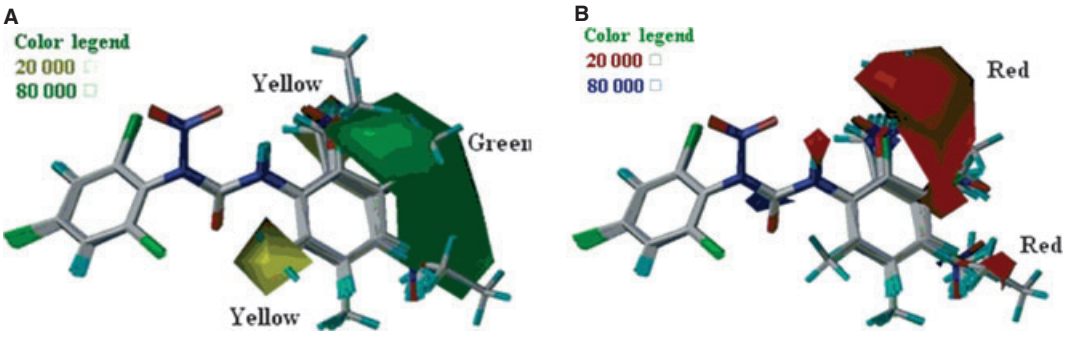

Figure 4: CoMSIA contour maps: (A) steric contour map; (B) electrostatic contour map.

The predicted and residual pIC_{50} values for the training and testing set compounds are listed in Table 3. The relative plots of the predicted versus experimental pIC_{50} values for the two models are shown in Figure 2. The average residual values for the test set of two models were 0.14 and 0.16. The external testing set yields a predictive R^2_{pred} of 0.662 and 0.568 for CoMFA and CoMSIA models. As seen, the values indicate that CoMFA and CoMSIA models possess a high predictive capacity, and the CoMFA model is considered more predictability with higher q^2, r^2, and R^2_{pred} than the CoMSIA model. So we could predict that the hydrogen bond is not the key element for the activity of these inhibitors.

The steric and electrostatic contribution contour maps of the best models of CoMFA and CoMSIA are plotted in Figures 3 and 4. In the steric contour maps, the green contours (80% contribution) represent regions that bulky substituents would increase the inhibitory activity, while the yellow contours (20% contributions) represent regions that steric bukly group would be unfavorable. While in the electrostatic contour maps, the blue and red contours (80% and 20% contributions) signify the position where positively charged groups and negatively charged groups would be favorable, respectively.

As shown in CoMFA steric map (Figure 3A), a bulky group in the region of the green contour on 4-position of *N*′-phenyl is favorable for activity. By comparing the structures and activities of 4-substituted compounds **4** (4-H), **5** (4-CH_3), **8** (4-NO_2), and **12** (4-Br), the activity order is: **8**>**12**>**5**>**4**, which coincides with the model prediction. The yellow contours near 2-position suggests that the smaller substituents on this region would be advantageous. It can be proven by the compounds **7**, **11,** and **17** with lower activity.

In the CoMFA electrostatic contour map (Figure 3B), a red and blue contour are, respectively, distributed before and behind the *N*′-phenyl ring. On the 2-position, there is red contour before the ring and also blue contour behind it, which indicates that both electropositive and electronegative group here benefit activity, such as compounds **9** (2-NO_2, pIC_{50} = 3.83), **11** (2-CH_3, pIC_{50} = 3.49), **27** (2-F, pIC_{50} = 4.36), and **40** (2-Cl, pCI_{50} = 4.26) result better inhibitory activity than compound **4** (2-H, pIC_{50} = 3.35). There is a bulky blue contour near 4,5-position, which shows electropositive groups here would benefit activity. For example, compounds **8** (4-NO_2), **13** (4-F), and **38** (4-Cl) possess significant inhibitory activity. And near 6-position, a red contour indicates electronegative groups are needed here. The CoMFA steric and electrostatic contour maps show that the linkers composed of small substituents on 2-position, bulky and electropositive groups on 4,5-region, electronegative groups on 6-position may increase the activity.

In Figure 4A, CoMSIA steric contour map, there is a big green contour covering all of the 2, 3, 4-position and two small yellow contours covering on the 2-region behind the ring and 6-position, respectively. So bulky groups linked to 3, 4-position of *N*′-phenyl ring may increase the activity, such as compounds **23** (3-Cl-4-CH_3, pIC_{50} = 4.14), **24** (3,4-di-CH_3, pIC_{50} = 4.08), **26** (3,4-di-OCH_3, pIC_{50} = 3.98), **32** (2,4-di-Cl, pIC_{50} = 4.24), and **41** (2-NO_2-4-Cl, pIC_{50} = 4.49). But near 2, 6-position suggests that substituents on this region would be small. It can be proven by compound **15**(2, 6-di-CH_3, pIC_{50} = 3.01) with lower activity.

Moreover, in the CoMSIA electrostatic contour map (Figure 4B), there are two bulky red contours near 2, 3-position before and behind the phenyl ring, which indicates that electronegative groups here benefits the activity, the CoMSIA steric and electrostatic contour maps indicate that linkers composed of small and electronegative groups on 2-position, bulky and electronegative substituents on 3-position, bulky groups on 4-region, small groups on 6-position may increase the activity.

Conclusions

Using a simple and convenient BTC one-pot synthetic method, we have prepared 38 *N*-nitrourea derivatives, and compounds **27**, **37**, **38**, **40**, and **41** exhibited excellent antifungal activities. Based on the experimental data, two best CoMFA and CoMSIA models with the cross-validated (LOO) q^2 values of 0.773 and 0.72 and no validated r^2 values of 0.959 and 0.936 were obtained, respectively. The testing set of compounds that gave a predictive R^2_{pred} of 0.662 and 0.568 for CoMFA and CoMSIA models indicate that the two best models could be effectively used to predict the activity of new inhibitors and guide the further modification of these compounds, just as small and electronegative groups on 2-position (2-F), bulky and electronegative substituents on 3-position (3-CF_3, 3-NO_2), bulky and electropositive groups on 4,5-region, and small and electronegative groups on 6-position may increase the activity.

Acknowledgements

We gratefully acknowledge the support of this work by the Fundamental Research Funds for the Central Universities (2010JC001) and the National Natural Science Foundation of China (31101467).

References

1. Duan G.F., Zhang Z.B., Zhang J.P., Zhou Y.G., Yu L.Q., Yuan Q.S. (2007) Evaluation of crude toxin and metabolite produced by *Helminthosporium gramineum* Rabenh for the control of rice sheath blight in paddy fields. Crop Prot;26: 1036–1041.
2. Groth D.E. (2008) Effects of cultivar resistance and single fungicide application on rice sheath blight, yield, and quality. Crop Prot;27:1125–1130.
3. Zhang C.Q., Liu Y.H., Ma X.Y., Feng Z., Ma Z.H. (2009) Characterization of sensitivity of Rhizoctonia solani, causing rice sheath blight, to mepronil and boscalid. Crop Prot;28:381–386.
4. Ren C.M., Gao B.D., He Y.C. (2001) Progress in the studies on *Rhizoctonia solani*. Plant Prot;27:32–36.
5. Yonova P.A., Stoilkova G.M. (2004) Synthesis and biological activity of urea and thiourea derivatives from 2-aminoheterocyclic compounds. J Plant Growth Regul;23:280–291.

6. Khan S.A., Singh N., Saleem K. (2008) Synthesis, characterization and in vitro antibacterial activity of thiourea and urea derivatives of steroids. Eur J Med Chem;43:2272–2277.
7. Džimbeg G., Zorc B., Kralj M., Ester K., Pavelic K., Andrei G., Snoeck R., Balzarini J., De Clercq E., Mintas M. (2008) The novel primaquine derivatives of N-alkyl, cycloalkyl or aryl urea: synthesis, cytostatic and antiviral activity evaluations. Eur J Med Chem;43:1180–1187.
8. Khan K.M., Saeed S., Ali M., Gohar M., Zahid J., Khan A., Perveen S., Choudhar M.I. (2009) Unsymmetrically disubstituted urea derivatives: a potent class of antiglycating agents. Bioorg Med Chem;17:2447–2451.
9. Zheng Q., Cheng K., Zhang X., Liu K., Jiao Q., Zhu H. (2010) Synthesis of some N-alkyl substituted urea derivatives as antibacterial and antifungal agents. Eur J Med Chem;45: 3207–3212.
10. Sun M., Wu X., Chen J., Cai J., Cao M., Ji M. (2010) Design, synthesis, and in vitro antitumor evaluation of novel diaryl ureas derivatives. Eur J Med Chem;45:2299–2306.
11. Sun C., Zhang X., Huang H., Zhou P. (2006) Synthesis and evaluation of a new series of substituted acyl(thio)urea and thiadiazolo [2,3-*a*] pyrimidine derivatives as potent inhibitors of influenza virus neuraminidase. Bioorg Med Chem;14:8574–8581.
12. Cross B., Hill R., Gastrock W.H. (1974) Phenylnitramine herbicides. US 3844762.
13. Cross B., Dawe D.H. (1978) Fungicidal phenylnitramines and new phenylnitramines. US 4130645.
14. Cross B., Bhalla P.R., O'Neal T.D. (1979) Substituted phenylnitramines with plant growth regulating properties. EP 0003880A1.
15. Cramer R.D., Patterson D.E., Bunce J.D. (1988) Comparative molecular field analysis (CoMFA). 1. Effect of shape on binding of steroids to carrier proteins. J Am Chem Soc;110:5959–5967.
16. Klebe G., Abraham U., Mietzner T. (1994) Molecular similarity indices in a comparative analysis (CoMSIA) of drug molecules to correlate and predict their biological activity. J Med Chem;37:4130–4146.
17. Kraim K., Khatmi D., Saihi Y., Ferkous F., Brahimi M. (2009) Quantitative structure activity relationship for the computational prediction of α-glucosidase inhibitory. Chemometrics Intell Lab Syst;97:118–126.
18. Ibrahim M.A., Abdel-Rahman R.M., Abdel-Halim A.M., Ibrahim S.S., Allimony H.A. (2009) Synthesis, chemical reactivity and fungicidal activity of pyrido[1,2-b][1,2,4]triazine derivatives. J Braz Chem Soc;20:1275–1286.
19. Qin J., Liu H., Li J., Ren Y., Yao X., Liu M. (2009) 3D-QSAR studies on the inhibitors of AP-1 and NF-κB mediated transcriptional activation. Eur J Med Chem;44:2888–2895.
20. Clark M., Cramer R.D. III, Van Opdenbosch N. (1989) Validation of the general purpose tripos 5.2 force field. J Comput Chem;10:982–1012.
21. Gasteiger J., Marsili M. (1980) Iterative partial equalization of orbital electronegativity-a rapid access to atomic charges. Tetrahedron;36:3219–3228.
22. Pick A., Müller H., Wiese M. (2008) Structure-activity relationships of new inhibitors of breast cancer resistance protein (ABCG2). Bioorg Med Chem;16:8224–8236.
23. Müller H., Pajeva I., Globisch C., Wiese M. (2008) Functional assay and structure-activity relationships of new 3rd generation P-glycoprotein inhibitors. Bioorg Med Chem;16:2448–2462.
24. Halgren T.A. (1990) Maximally diagonal force constants in dependent angle-bending coordinates. II. Implications for the design of empirical force fields. J Am Chem Soc;112:4710–4723.
25. Liao S., Qian L., Miao T., Lu H., Zheng K. (2009) CoMFA and docking studies of 2-phenylindole derivatives with anticancer activity. Eur J Med Chem;44:2822–2827.
26. Lobanova A.A., Il'yasov S.G., Popov N.I., Sataev R.R. (2002) Chemistry of urea nitro derivatives: II. Synthesis of nitramide from N,N'-dinitrourea. New reactions of nitramide. Russ J Org Chem;38:1–6.
27. Gool M.V., Bartolomé J.M., Macdonald G.J. (2008) An easy and versatile synthesis of ureas from 2-benzyl aminopyrimidine. Tetrahedron Lett;49:7171–7173.